JOURNAL OF MATERIALS SCIENCE **39** (2004) 1267– 1276

Effects of thickness and environmental temperature on fracture behaviour of polyetherimide (PEI)

KI-YOUNG KIM, LIN YE*
Center for Advanced Materials Technology, School of Aerospace, Mechanical and Mechatronic Engineering, The University of Sydney, Sydney, NSW 2006, Australia
E-mail: kykim@aeromech.usyd.edu.au
E-mail: ye@aeromech.usyd.edu.au

The fracture behaviour of a polyetherimide (PEI) thermoplastic polymer was studied using compact tension (CT) specimens with a special emphasis on effects of specimen thickness and testing temperatures on the plane strain fracture toughness. The results show that the valid fracture toughness of the critical stress intensity factor, K_{IC}, and strain energy release rate, G_{IC}, is independent of the specimen thickness when it is larger than 5 mm at ambient temperature. On the other hand, the fracture toughness is relatively sensitive to testing temperatures. The K_{IC} value remains almost constant, 3.5 MPa$\sqrt{m}$ in a temperature range from 25 to 130°C, but the G_{IC} value slightly increases due to the decrease in Young's modulus and yield stress with increasing temperature. The temperature dependence of the fracture toughness, G_{IC}, was explained in terms of a plastic deformation zone around the crack tip and fracture surface morphology. It was identified that the larger plastic zone and extensive plastic deformation in the crack initiation region were associated with the enhanced G_{IC} at elevated temperatures.

1. Introduction

As many polymeric materials have been considered as matrix resins for fibre reinforced composites and structural adhesives in various aerospace and automobile applications, it is becoming important to understand the fracture behaviour of polymers and to acquire the quantitative information on intrinsic fracture toughness that can be used in engineering design. The application of linear elastic fracture mechanics (LEFM) parameters such as the critical stress intensity factor, K_{IC} and strain energy release rate, G_{IC} to characterise fracture toughness for polymers is standardised and now well documented [1]. The K_{IC} and G_{IC} values measured from LEFM are successfully applied to evaluate the plan-strain fracture toughness if the plastic zone at the crack tip is small compared to the relevant specimen dimension (e.g., thickness and width). In the plane-strain state, yielding along the crack tip line in the thickness direction is constrained by the surrounding undeformed materials, leading to a brittle fracture mode and a lower bound value of fracture toughness [2, 3]. On the other hand, if extensive plastic deformation occurs at the crack tip, a relatively large and thick specimen is required for the valid plane-strain fracture toughness. Otherwise, extensive yielding can take place in the thickness direction, leading to a plane stress condition, invalidating LEFM and overestimating fracture toughness. Although the requirement of the large and thick specimen to ensure the plane strain state is experimentally expensive and laborious, the measurement of the plane strain fracture toughness can provide comparative and/or intrinsic values in toughness for engineering design.

Polyetherimide (PEI) is a high performance amorphous thermoplastic polymer, which is used not only for thermoplastic matrix composites, but also for engineering applications in bulk and adhesive forms. However, fracture mechanisms and toughness data are limited to the open literature, to the authors' knowledge, especially with respect to environmental testing temperatures. The objective of this study is to measure the plane strain fracture toughness of a PEI thermoplastic polymer in a temperature range from room temperature (RT, approximately 25°C) to 130°C. In addition, influences of specimen thickness on fracture behaviour are investigated. It is well recognised that loading rates also have a significant effect on fracture toughness due to the viscoelastic/plastic properties of polymeric materials [4]. However, this dependence is not investigated in the present study, which mainly is concerned with temperature effects on fracture mechanisms and the plane-strain fracture toughness of the PEI polymer.

*Author to whom all correspondence should be addressed.

2. Experimental

2.1. Materials

Commercial grade PEI pellets (ULTEM 1000, supplied by GE Plastics) were used and dried at 150°C for 5 h to remove moisture prior to compression moulding. A rectangular flat mould was used to manufacture PEI panels. The internal dimension of the cavity of the mould is 200 × 200 mm and the plate thickness could be adjusted by changing the amount of PEI pellets, so the PEI panels of a thickness of 4, 6, 12 and 22 mm, respectively, were manufactured.

After the mould was cleaned with acetone, Frekote® release agent was applied to the internal surface of the mould to ensure that the resin would not adhere to the tooling surface. The dried pellets in the closed mould were first preheated at 320°C for 1 h, and then a compression pressure of 0.5 MPa was applied for 30 min. The mould was cooled under the pressure to a temperature far below a glass transition temperature of 217°C.

2.2. Tensile tests

Tensile tests were performed in accordance with ASTM D 638-99 [5], expect that the uniform section specimen was replaced with an hour-glass specimen [6] of 4 mm in thickness, shown in Fig. 1a. The tensile tests were carried out at a crosshead speed of 2 mm/min at temperatures of RT, 80 and 130°C using an environmental chamber on an Instron 5567 universal testing machine with a computer data acquisition system. Strains were measured using a clip gauge with a 25 mm gauge length at RT. At elevated temperatures, strains measured from machine displacements were calibrated with those from the clip gauge measurement at RT. Stresses were calculated dividing the load by the original cross-sectional area, and Young's modulus and yield stress were determined from the slope of the initial straight line and the maximum stress of the stress-stress curves, respectively.

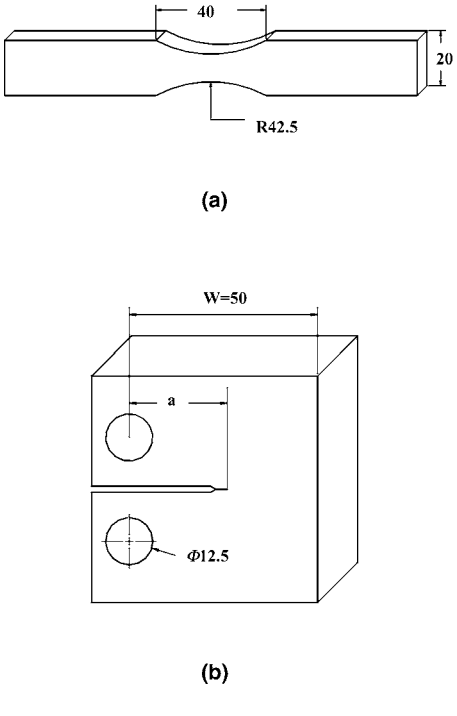

Figure 1 Specimen geometry for characterisation of mechanical properties: (a) tensile specimen and (b) compact tension (CT) specimen (all dimensions in mm).

2.3. Compact tension tests

The PEI panels with a thickness of 6, 12 and 22 mm were machined into compact tension (CT) specimens, shown in Fig. 1b. The CT specimens were carefully pre-cracked from the machined notch using a razor blade tapping method to produce a sufficiently sharp notch [7], and the length of the initial crack, a/W, was controlled between 0.45 and 0.55. Compact tension tests were performed at temperatures of RT, 80 and 130°C, respectively, at a crosshead speed of 10 mm/min using an environmental chamber. According to ASTM D 5045-99 [1], the fracture toughness for the CT specimen is calculated using:

$$K_{\mathrm{Q}} = \frac{P}{BW^{1/2}} f(x) \tag{1}$$

where P is either the maximum load or the load at the intercept of the 95% slope for the load-displacement curve, and in this study the maximum load was used; B is the specimen thickness, and $f(x)$ is a function of the ratio of the crack length to the specimen width, $x = a/W$, defined by:

$$f(x) = \frac{(2+x)(0.886+4.64x-13.32x^2+14.72x^3-5.6x^4)}{(1-x)^{3/2}} \tag{2}$$

K_{Q} is equal to the plane-strain fracture toughness, K_{IC}, if the following criteria are satisfied:

$$B, a, (W-a) > 2.5(K_{\mathrm{Q}}/\sigma_{\mathrm{y}})^2 \tag{3}$$

where σ_{y} is the yield stress. K_{IC} can be used to obtain the critical strain energy release rate, G_{IC}, from

$$G_{\mathrm{IC}} = \frac{(1-v^2)K_{\mathrm{IC}}^2}{E} \tag{4}$$

where v is Poisson ratio and E is Young's modulus; v is set to 0.4 in the calculation. For both tensile and compact tension tests, at least 3 specimens were tested for each testing temperature, and the averaged results are reported.

2.4. Fractographic analysis

The scanning electron microscopy (SEM) study was performed on Philips SEM505 with an accelerating voltage of 10 kV to examine fracture surfaces of the CT specimens. The fracture surfaces were sputter-coated with gold before fractographic study. For all micrographs shown in this study, the main crack direction is always from left to right.

TABLE I Tensile properties of PEI specimen as a function of temperature

Temperature (°C)	Young's modulus (GPa)	Yield strength (MPa)
25	3.3	111
80	2.7	87
130	2.5	64

3. Results and discussion

3.1. Tensile properties

The tensile properties of the PEI polymer are summarised in Table I. Both Young's modulus and yield stress decrease with an increase in temperature. The modulus values agree with those reported in other work [8] despite a difference in specimen geometry. In general, it is well known that the modulus and yield stress decrease with increasing temperature and decreasing strain rates for all polymers including thermoset, semicrystalline and amorphous thermoplastic polymers [9]. For the amorphous thermoplastic polymers such as PEI, these phenomena can be explained in terms of the molecular segments mobility and molecular interaction. The mobility depends on physical and chemical bonds as well as bulky side groups. With increasing temperature, vibration between molecular chains increases as does the size of the empty spaces between the chains, weakening the molecular interaction and facilitating the rearrangement process of the molecules. If the loading period is short compared with the time taken for the molecular rearrangement, the polymeric materials will be rigid and brittle. If, on the other hand, the rearrangement mechanisms are able to cope with the applied loads within the period of loading until an equilibrium value is reached, the material will be flexible and tough. Therefore, the polymeric materials can exhibit either brittle or tough deformation behaviour at different temperatures and loading speeds [10].

3.2. Fracture behaviour

3.2.1. Crack propagation modes

Typical load-displacement curves from the CT tests are shown in Fig. 2, demonstrating thickness and temperature effects on crack growth behaviour. In the load-displacement curves, the sudden load-drop indicates the fast unstable crack growth because additional energy is not required. However, the load drops gradually at elevated temperatures, indicating additional crack opening displacement is required for crack propagation, and hence the crack propagation becomes slower and more stable. Three different crack propagation modes are observed macroscopically, viz. unstable (fast), stable (slow), and stable/unstable, which were identified for other thermoplastic polymers [11]. Under a certain condition, e.g., 12 mm thick specimens at 80°C and 22 mm thick specimens at 130°C, a typical stable/unstable crack propagation mode was observed. The crack initially propagated in a stable manner, but eventually in an unstable manner with a transition point marked by the sharp load drop after the gradual load decrease in the load–displacement curves. With different specimen thickness and testing temperatures, the crack propagation mode is summarised in Table II. The PEI specimen shows a general trend that the crack growth becomes more stable by decreasing specimen thickness or increasing testing temperatures. These observations are in good agreement with those for other glassy thermoplastic polymers [12].

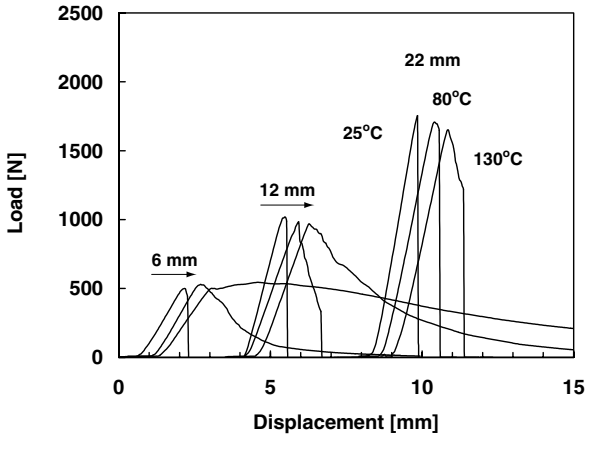

Figure 2 Thickness and temperature effects on load-displacement curves of PEI polymer in CT fracture tests. Arrows indicate increasing temperature from RT, 80 and 130°C.

3.2.2. Fracture surfaces

The photographs of fracture surfaces in Fig. 3 show that CT specimens fractured in three different modes such as brittle, brittle with shear lips and ductile fracture, depending on specimen thickness and testing temperatures. These fracture modes are similar to those of the previous reports for glassy polymers in impact [12] and CT fracture [13] tests. The shear lip is formed as a result of the change of the stress state from triaxial tension (plane strain) in the central region of the specimens to a biaxial one (plane stress) in the surface regions. Accordingly, the central region of the specimens fractures in a brittle mode, while the surface regions show a ductile yielding with the lateral contraction. The extent and width of shear lips were dependent on the testing temperature. The formation of shear lips at both edges of the fracture surface was more favored at high temperatures, increasing the crack stability and suppressing unstable crack growth. The fracture surface of the 6 mm specimen tested at 130°C, which did not satisfy the ASTM size criteria, reveals a typical example of the ductile plane stress fracture mode with a triangle rough whitened front zone and greater lateral contraction zones along the fracture surface. However, at RT, all specimens fractured in a brittle unstable manner at the maximum load without shear lips. Although the unstable fracture results in relatively flat fracture surfaces, optically three distinct zones can be identified including a rough whitened front zone, a hazy middle zone and a flat darkened rear zone, as shown in Fig. 3. The morphological change in the fracture surface implies that major microscopic fracture mechanisms at crack initiation are quite different from those during crack growth. Three characteristic zones were also identified for other thermoplastics [13, 14]. In particular, the three

TABLE II Plastic deformation zone size and crack growth modes of PEI polymer at different temperatures

Thickness (mm)	Temperature (°C)	Crack growth mode	Ductility factor	Plastic zone size (mm)		
				Plane stress	Plane strain	Dugdale
6	25	Unstable	0.0010	0.16	0.05	0.40
	80	Stable	0.0017	0.28	0.09	0.70
	130	Stable/necking	0.0064	1.03	0.34	2.54
12	25	Unstable	0.0010	0.17	0.05	0.41
	80	Stable/unstable	0.0016	0.25	0.08	0.62
	130	Stable	0.0030	0.47	0.15	1.17
22	25	Unstable	0.0010	0.16	0.05	0.39
	80	Unstable	0.0016	0.25	0.09	0.62
	130	Stable/unstable	0.0030	0.47	0.16	1.16

(a)

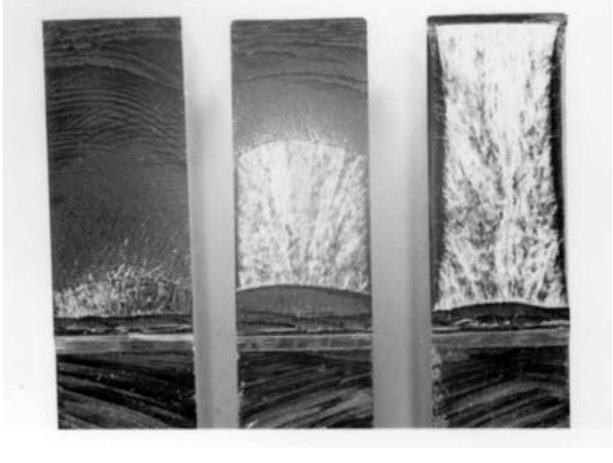

(b)

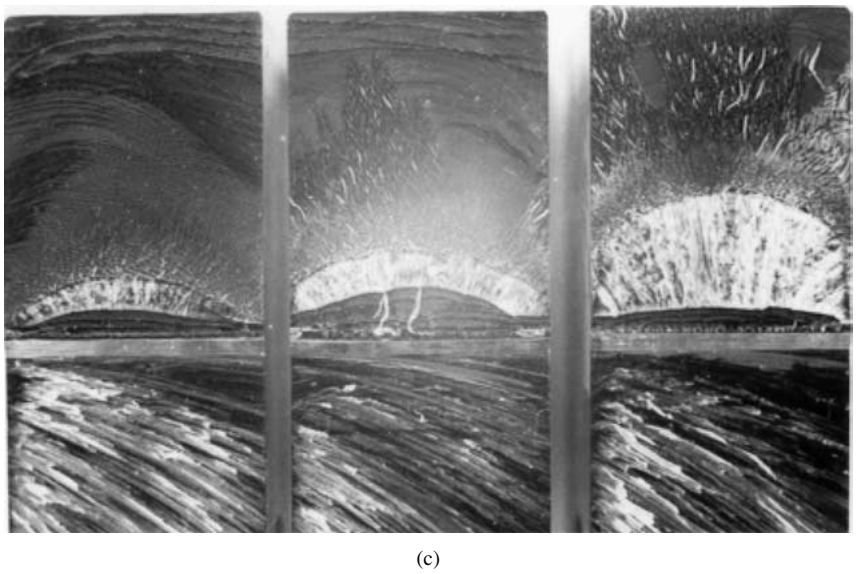

(c)

Figure 3 Fracture surfaces of PEI polymer of different thickness tested at RT, 80 and 130°C from the left to right direction: (a) 6 mm, (b) 12 mm, and (c) 22 mm.

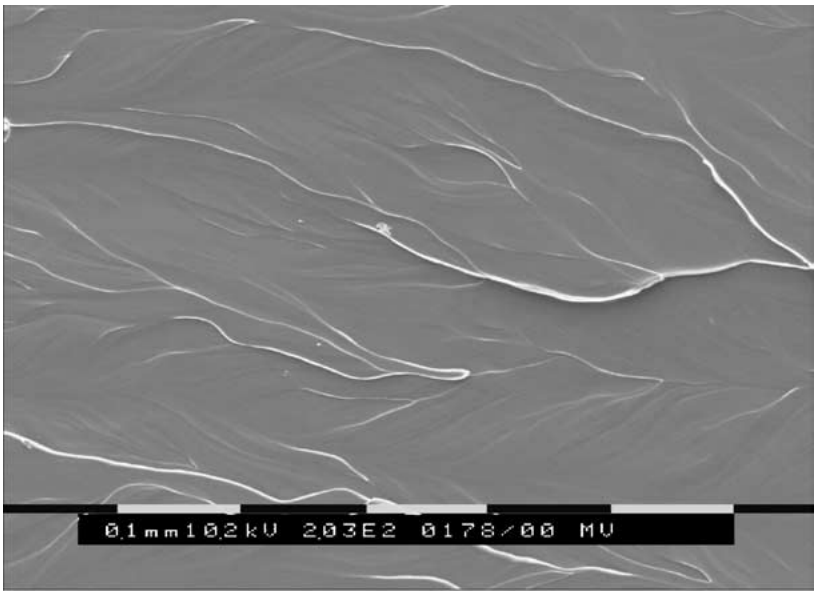

(a)

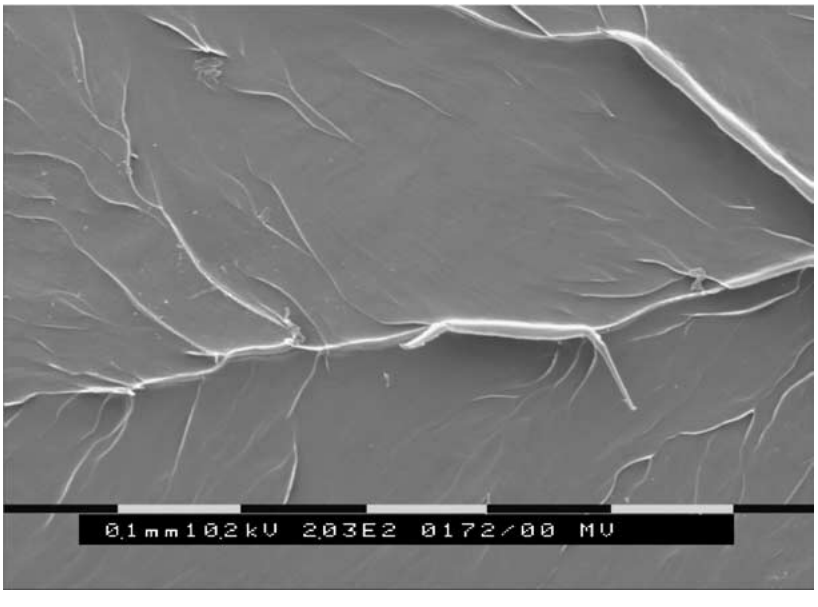

(b)

Figure 4 Microflow lines and river patterns in rough whitened front zone (initiation region) of fracture surfaces of PEI polymer at different testing temperatures: (a) RT and (b) 130°C.

fracture zones, corresponding to crack initiation, mist and mirror/end regions respectively, were identified on fast unstable fracture surfaces of a polycarbonate in impact [15] and in tension [16].

The SEM micrograph of the rough whitened front zone shows that the crack initiation region consists mainly of microflow lines and ridges commonly known as a river pattern, shown in Fig. 4. The river pattern is commonly observed in brittle fracture surfaces of metals, ceramics and polymers as a result of the progressive joining and reorientation of various cleavage crack planes during the crack growth [17]. For glassy thermoplastic polymers, the river pattern can be formed by the coalescence of crazes simultaneously having developed on different planes and then separation of the multiple crazes [14]. Crazing is one of primary localised plastic deformation mechanisms in glassy polymers. In general, crazing initiates with the nucleation of microvoids in areas of stress concentration, but prevents the coalescence of these voids and fracture by stretching fibrils from bulk materials and creating a crack like void-fibril structure. After further craze widening, the fibrils start gradually to breakdown with slow stable crack extension prior to an unstable crack propagation, and hence crazing can be considered as a precursor to unstable brittle fracture [4, 18]. Since the process of craze initiation, widening and breakdown in the initiation region involves a significant amount of plastic deformation and energy absorption, crazing formation is a relatively high energy-consuming process, and plays a decisive role in the fracture toughness of glassy polymers [16]. Also, the formation of the river patterns can give valuable information for determining the macroscopic crack growth direction [19], shown in Fig. 4, where the coalescence direction of the microflow and river pattern lines coincides with the crack growth direction from left

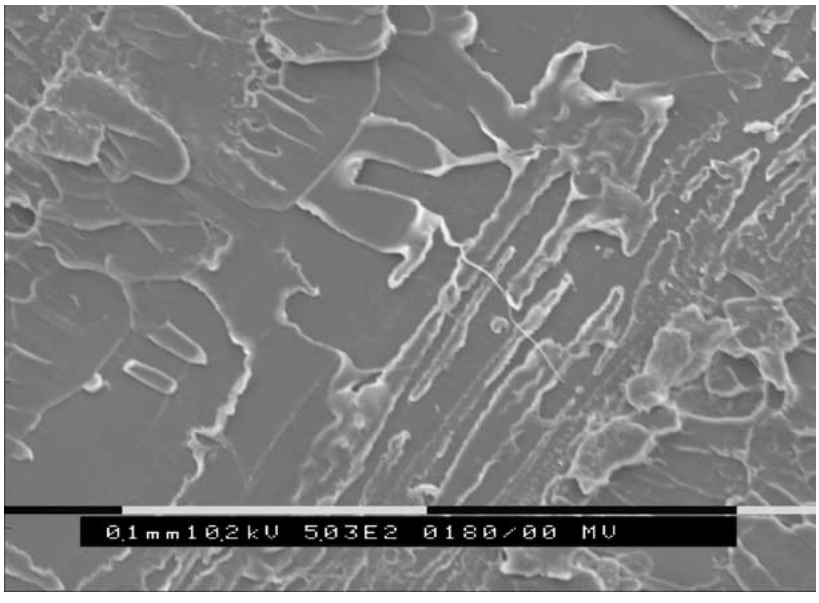

Figure 5 Patch patterns in a hazy middle zone (mist region) of fracture surface of PEI polymer tested at RT.

to right. Beyond the initiation region, the hazy middle zone (a mist region) optically exhibits smoother fracture surfaces with less plastic deformation (crazing). Microscopically, the region consists of small island structures of protruding and recessed craze materials on one or other of the fracture surfaces, giving rise to a distinctive morphological feature of patch patterns, illustrated in Fig. 5. The patch pattern resulted from the crack oscillating between two craze/bulk polymer interfaces because the craze had not enough time to grow in thickness during the fast crack propagation [4, 16]. Although river patterns is observed in the start of the mist region, the patch pattern is the most distinctive morphological feature in the mist region for the specimens tested at RT. The change in fracture morphology from the initiation region to the mist region corresponds to the onset of the unstable fast crack growth, which is marked as an abrupt load drop in the load-displacement curve. Such crack instability can be attributed to the increased driving force for the unstable crack growth because a greater excess of energy would be stored as a result of the stable crack growth in the initiation region and available to accelerate the crack growth rapidly [14]. In the end of the fracture surface, the flat darkened zone exhibits optically smoothest and most featureless surfaces, but the high magnification SEM micrograph in Fig. 6 shows end-banded structures, where end bands are evenly spaced and oriented perpendicular to the direction of local crack propagation front with island structures of crazed materials. However, in this region, elongated conical markings, which were identified in the mirror region for fracture of a polycarbonate by other researchers [16], could not be found in this study.

The initiation region of the specimens tested at 130°C is characterised by more distinctive and thicker river patterns (Fig. 4b), which would be reflected on more surface roughness (whitening) in the whitened front

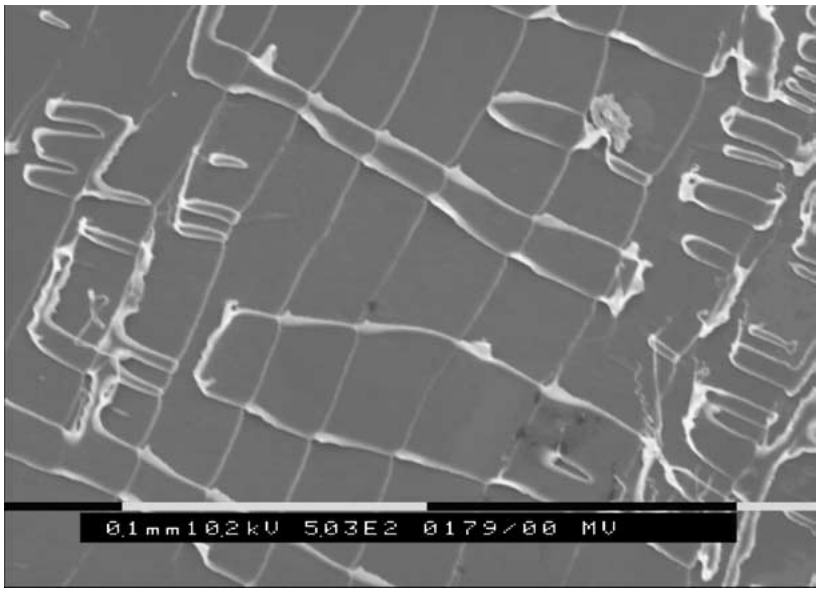

Figure 6 End-banded structures in a flat darker-colored rear zone (mirror/end band region) of fracture surface of PEI polymer tested at RT.

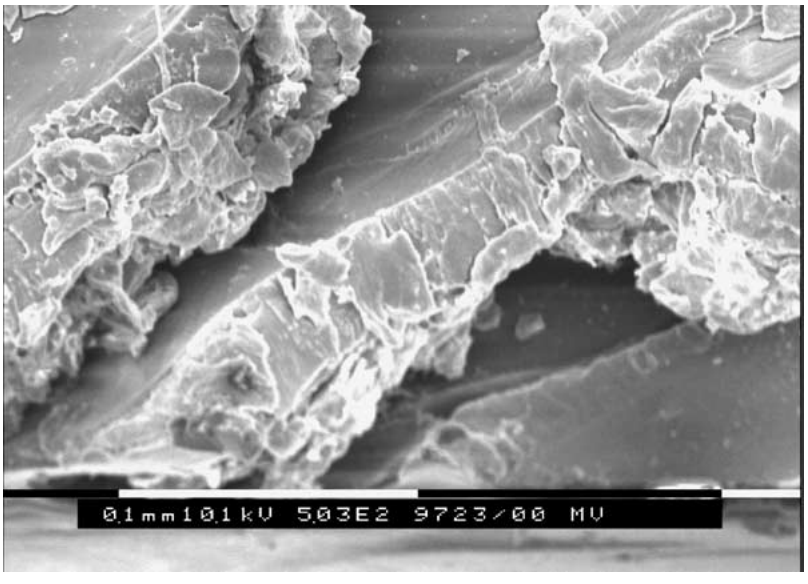

Figure 7 Shear lip region of PEI polymer tested at 130°C.

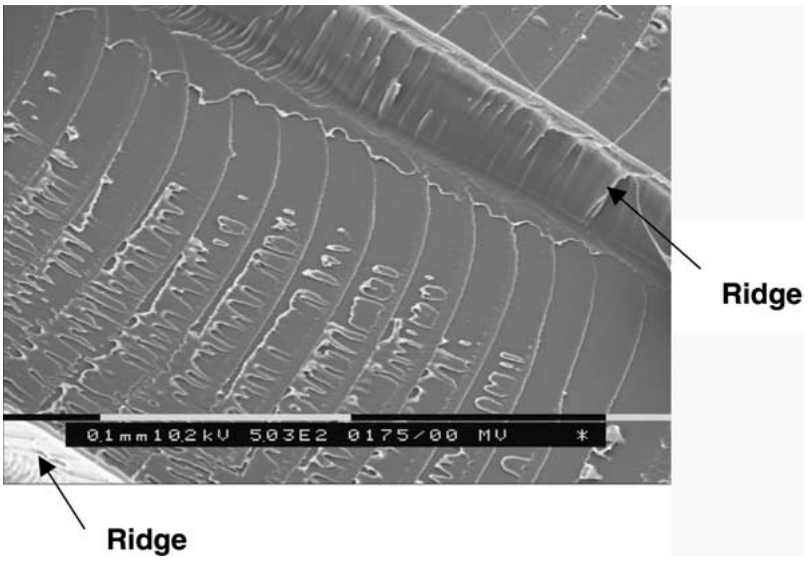

Figure 8 Ridges and end-banded structures in a hazy middle zone (mist region) of fracture surface of PEI polymer tested at 130°C.

zone. In contrast to the absence of shear lips in the specimens tested at RT, the initiation region includes the additional fracture region of shear lips near the edges of the surface areas. The microscopic examination of the fracture region shows a very rough surface with extensive tearing-type shear deformation, shown in Fig. 7. The mist region also shows the morphology different from that at RT. Fig. 8 shows that the ridges extend from the initiation region through the mist region, but its density is less than those in the initiation region. The fracture surface between the ridges shows the brittle fracture surface characterised by many microflow lines and end-banded structures. The ridge formation becomes the dominant feature in the mist region instead of patch patterns observed at RT, and appears to require significant energy absorption to propagate the crack. However, the transition from the initiation region to the mist region in the fracture surface indicates the onset of the unstable fast fracture following the stable crack propagation, which is marked as an abrupt load drop after the gradual decrease in the load-displacement curve, similarly to the corresponding transition observed in the fracture surface at RT.

The extent (size) and roughness of each fracture region appears to be a result of the combination of specimen thickness and testing temperatures. As the temperature increases and the specimen thickness decreases, the extent and roughness of the rough whitened front zone (crack initiation region) and hazy middle zone (mist region) increase while those of the flat darker rear zone (mirror/end band region) decrease, as shown in Fig. 3. Especially, the whitened zone shows a more increasing propensity. For the specimens with 6 and 12 mm in thickness tested at 80 and 130°C respectively, the whitened zone spreads throughout the whole fracture surface and shear lips forms along the both edges of the fracture surface. This uniformly rough fracture surface indicates the stable crack propagation without crack instability, as evidenced by the gradual decrease in the load-displacement curves. Elevated temperatures decrease crazing and yield stresses, promoting local plastic deformation through crazing or

yielding around the crack tip, depending on the stress state, due to easy movement of molecular chains of the PEI polymer. Thus, elevated temperatures would increase the size of craze zone (craze width and length) during stable crack growth because fast brittle fracture is impeded by crazing and yielding [20]. Therefore, the extent and roughness of the crack initiation region increased with increasing temperature. The extensive deformation of crazing and yielding in the crack initiation region would consume more energy and be reflected on greater fracture toughness of the PEI polymer at elevated temperatures.

3.3. Fracture toughness

3.3.1. Thickness effect

The effects of specimen thickness on fracture behaviour of thermoplastic polymers such as polyethylene (PE), polymethylmethacrlylate (PMMA), polycarbonate (PC) and polyethersulphone (PES) has been extensively investigated by various researchers [2, 21–23]. It was demonstrated that for sufficiently thick specimens, fracture toughness is independent of thickness because surface regions, where a plane stress state exists, are relatively small and their influence is neglectable. However, in thin specimens, the plane stress region is not small in comparison with the plane strain region, and hence the fracture toughness is dependent on the relevant ratio between the size of the plane stress and plane strain regions.

The specimen thickness effect on fracture toughness, K_Q, of the PEI polymer is shown in Fig. 9. The K_Q value is equal to the critical plane strain fracture toughness, K_{IC}, if the specimen thickness satisfies the ASTM thickness requirement. The minimum thickness is calculated using Equation 3, where the average K_Q value and yield stress are used. This is displayed as a dotted line in Fig. 9, and only the 6 mm specimen tested at 130°C did not satisfy the size requirement. The loss of the plane strain condition and attainment of the plane-stress condition leads to a clearly higher K_Q value in the tested temperature range. The valid plane-strain fracture toughness, K_{IC}, of the PEI polymer shows the same trend as other thermoplastic polymers that an approximately constant value is obtained independently of the specimen thickness.

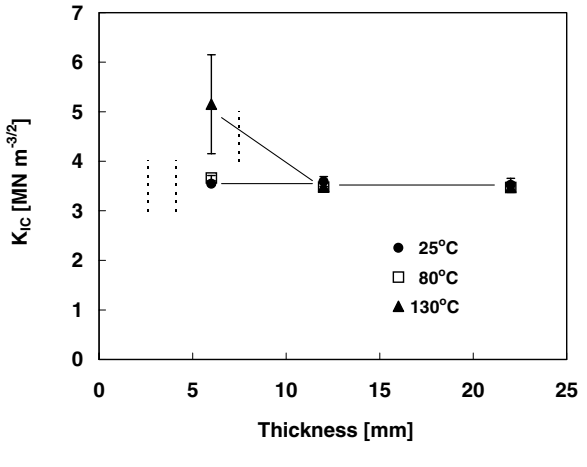

Figure 9 Thickness effect on fracture toughness, K_{IC} of PEI polymer with different specimen thickness at different testing temperatures. The dotted lines indicate the ASTM thickness requirement for K_{IC} at RT, 80 and 130°C (from left to right).

3.3.2. Temperature effect on fracture toughness

The environmental temperature has a considerable effect on fracture toughness, K_{IC} and G_{IC} for thermoplastic polymers because the polymers exhibit a transition from brittle to ductile as testing temperature increases. Fig. 10 shows the temperature effects on fracture toughness of the PEI polymer. The 6 mm thick specimen has almost same value as that for the thicker specimens at room temperature, but has a higher value at 80°C although the thickness satisfies the ASTM minimum thickness requirement at the temperature, shown in Fig. 9. It was reported that the ASTM thickness requirement does not provide the sufficient condition for valid plane strain fracture due to the lack of the constraint at the crack tip in CT specimens [2]. For 12 and 22 mm thick specimens, they have almost the same K_Q values with respect to testing temperatures. Such thickness independence indicates that the valid plane strain fracture toughness, K_{IC}, has been determined over the entire temperature range using the LEFM concept. Although K_{IC} remains almost constant, G_{IC} slightly increases with increasing temperature from RT

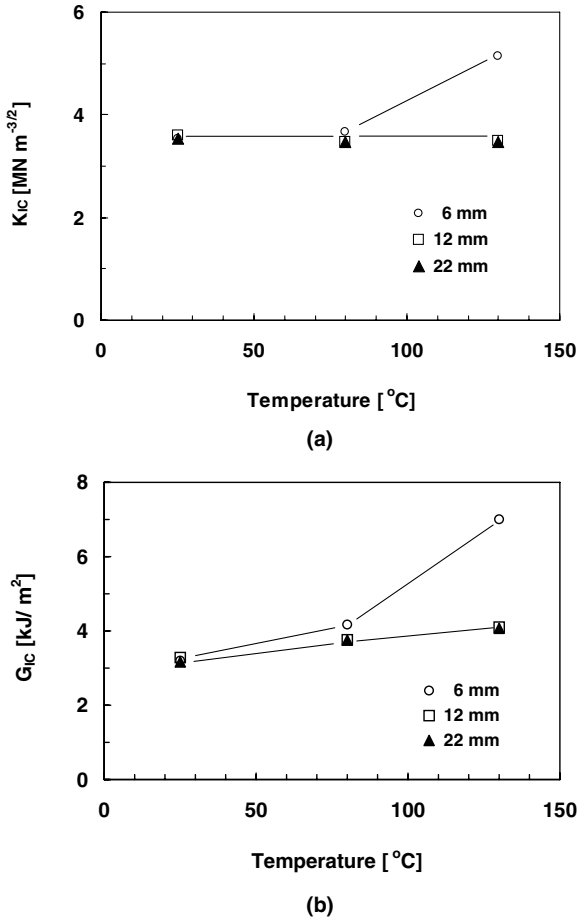

Figure 10 Temperature effect on fracture toughness of PEI polymer: (a) K_{IC} and (b) G_{IC}.

to 130°C. The increase in G_{IC} is attributed to the decreased Young's modulus at elevated temperatures because the critical strain energy release rate is inversely proportional to Young's modulus in the data reduction method (Equation 4). Using fracture data for the 12 mm thick CT specimens, G_{IC} was calculated from the integrated areas in the measured load-displacement curves in accordance of the procedure given in ASTM D 5045-99 [1]. The values of 3.27 ± 0.6, 3.94 ± 0.18 and 4.29 ± 0.14 kJ/m^2 at RT, 80 and 130°C, respectively, were obtained, which confirms that the fracture toughness, G_{IC}, increases with increasing temperature. These data are correlated with those reported by Frassine and Pavan [24] that G_{IC} increased with increasing temperature from 23 to 130°C at the same crack speed for PEI. However, this fracture behaviour is opposite to that of the brittle polymer PMMA reported by other investigators [25, 26], where the fracture toughness, both K_{IC} and G_{IC}, decreases as the testing temperature increases from −80°C and 80°C. It was also reported that K_{IC} of PMMA decreased with increasing temperature over the range from −35 to 60°C, but increased above 90°C, reaching a maximum at T_g and then dropped off with increasing temperature [27]. This similar trend of fracture toughness was observed for phenolphthalein polyether ketone (PEK-C) [28]. For ductile PC polymers, Parvin and Williams [22] found that the plane-strain fracture toughness was approximately independent of temperature below −40°C. The somewhat different results for a PC polymer were reported by Nimmer [29] that the toughness slightly increased with increasing temperature from −40 to −20°C. The dependence of fracture toughness of other thermoplastics were investigated including poly(phenylen oxide)(PPO), polysulfone (PS) and PC [30], and PEEK [31]. From the literature, it is difficult to infer the obvious generality of the temperature dependence of polymer fracture toughness because fracture behaviour is highly complicated due to their interrelated dependence on testing variables and material properties. For instance, the fracture behaviour changes from brittle to ductile, or vice versa in response to not only temperature, but also other numerous variables such as notch tip radius, specimen thickness and geometry, loading mode and rate, molecular weight, crystallinity, physical aging, etc. [12, 13].

As mentioned earlier, it was observed in this study that K_{IC} remained almost constant and G_{IC} slightly increased with increasing temperature from RT to 130°C. It was identified that the initiation and growth of craze-crack occurred prior to the maximum load point, providing a rough whitened front zone with the fracture surface of the PEI specimen tested at room temperature (Fig. 3). With increasing temperature, significant plastic deformation around the crack tip such as crazing and yielding can easily take place, and consequently the crack tip will be effectively blunted due to much more localized plastic deformation around the crack tip of the specimen. Hence, the development of plastic zone around the crack tip plays a very important role to control the measured fracture toughness and to determine the fracture mode whether brittle or ductile. The LEFM provides simple theoretical expressions for the plastic zone size:

$$r_p = \frac{1}{2\pi}\left(\frac{K_C}{\sigma_y}\right)^2 \quad \text{for plane stress} \tag{5}$$

$$r_p = \frac{1}{6\pi}\left(\frac{K_C}{\sigma_y}\right)^2 \quad \text{for plane strain} \tag{6}$$

$$R_p = \frac{\pi}{8}\left(\frac{K_C}{\sigma_y}\right)^2 \quad \text{Dugdale model} \tag{7}$$

where r_p is the radius of the plastic zone, and R_p is the length of the Dugdale plastic zone. For thermoplastic polymer materials, however, the plastic zone size, which cannot be uniquely described by one single expression, depends upon deformation mechanisms around the crack tip, e.g., crazing or shear yielding. Consequently, a ductility factor denoted by $(K_C/\sigma_y)^2$, which is the unique part of Equations 5–7, was introduced to describe the plastic zone size and to provide the quantitative relationship with fracture toughness [32]. The plastic zone size and ductility factor calculated from these equations show increasing values with increasing testing temperatures, shown in Table II, which correlates well with the measured G_{IC} at elevated temperatures.

4. Conclusions

The plane strain fracture toughness of a PEI thermoplastic polymer has been successfully determined in the temperature range from RT to 130°C. When the valid fracture toughness values were obtained, the effect of the specimen thickness on fracture toughness, K_{IC} or G_{IC}, was minimal. Meanwhile, the value of K_{IC} remains almost constant in the temperature range whereas G_{IC} slightly increases with increasing temperature. The controversial results were explained by counterbalance effects of decreased Young's modulus and promoted local plastic deformation with increasing temperature.

It was also identified that varying specimen thickness and testing temperature affected the crack propagation mode and fracture surface morphology. The crack growth became more stable when brittle fast fracture was inhibited by decreasing specimen thickness and increasing testing temperatures. The fracture surface was subdivided into a whitened front zone (crack initiation), a hazy middle zone (mist) and a flat darkened rear zone (mirror/end regions). The extent and roughness of the crack initiation and mist regions increased while that of the mirror/end band region decreased at elevated temperatures due to the decreased crazing and yield stresses, facilitating local plastic deformation through crazing or yielding around the crack tip.

Acknowledgement

The authors wish to thank to Dr. Cheng Yan at Center for Advanced Materials Technology of the University of Sydney for the helpful discussions in interpreting the experimental results.

References

1. "ASTM D 5045-99 Standard Test Methods for Plane-Strain Fracture Toughness and Strain Energy Release Rate of Plastic Materials" (American Society of Testing and Materials, Philadelphia, 1999).
2. S. HASHEMI and J. G. WILLIAMS, *J. Mater. Sci.* **19** (1984) 3746.
3. S. Y. HOBBS and R. C. BOPP, *Polymer* **21** (1980) 559.
4. A. J. KINLOCH and R. J. YOUNG, in "Fracture Behaviour of Polymers" (Elsevier, London, 1983) p. 26.
5. "ASTM D 638-99 Standard Test Methods for Tensile Properties of Plastics" (American Society of Testing and Materials, Philadelphia, 1999).
6. K. N. KNAPP II, G. A. GABRIELE and D. LEE, *ANTEC'97* (1997) 1198.
7. K. XIAO, L. YE and Y. S. KWOK, *J. Mater. Sci.* **33** (1998) 2831.
8. in "The Effect of Temperature and Other Factors on Plastics" (Plastics Design Library, New York, 1990) p. 275.
9. W. BROSTOW and R. D. CORNELIUSSEN, in "Failure of Plastics" (Hanser Publisher, Munich, 1986) p. 98.
10. L. ENGEL, "An Atlas of Polymer Damage: Surface Examination by Scanning Electron Microscope" (Wolfe Science, 1981) p.
11. L. YE, C. T. YUAN and Y. W. MAI, *Polym. Compos.* **19** (1998) 830.
12. H. R. BROWN, *J. Mater. Sci.* **17** (1982) 469.
13. F.-C. CHANG and W.-B. LIU, *J. Appl. Polym. Sci.* **44** (1992) 1615.
14. L. H. LEE, J. F. MANDELL and F. J. MCGARRY, *Polym. Eng. Sci.* **27** (1987) 1128.
15. D. HULL and T. W. OWEN, *J. Polym. Sci., Polym. Phy. Ed.* **11** (1973) 2039.
16. C. M. AGRAWAL and G. W. PEARSALL, *J. Mater. Sci.* **26** (1991) 1919.
17. G. W. POWELL, "Failure Analysis and Prevention," Vol. 11 (American Society for Metals, Metals Park, OH, USA, 1990) p. 75.
18. M. G. A. TIJSSENS, E. VAN DER GIESSEN and L. J. SLUYS, *Int. J. Solids Struct.* **37** (2000) 7307.
19. B. W. SMITH and R. A. GROVE, *ASTM STP* **948** (1987) 68.
20. W. DOLL and L. KONCZOL, *Adv. Polym. Sci.* **91/92** (1991) 138.
21. M. K. V. CHAN and J. G. WILLIAMS, *Polym. Eng. Sci.* **21** (1981) 1019.
22. M. PARVIN and J. G. WILLIAMS, *J. Mater. Sci.* **10** (1975) 1883.
23. P. J. HINE, R. A. DUCKETT and I. M. WARD, *Polymer* **22** (1981) 1745.
24. R. FRASSINE and A. PAVAN, *Compos. Sci. Technol.* **54** (1995) 193.
25. A. G. ATKINS, C. S. LEE and R. M. CADDELL, *J. Mater. Sci.* **10** (1975) 1381.
26. G. P. MARSHALL, L. H. COUTTS and J. G. WILLIAMS, *ibid.* **9** (1974) 1409.
27. K. MIZUTANI, *J. Mater. Sci. Lett.* **6** (1987) 915.
28. Y. HAN, Y. YANG, B. LI and Z. FENG, *J. Mater. Sci.* **30** (1995) 3658.
29. R. NIMMER, in "Engineered Materials Handbook," Vol. 2, Engineering Plastics (ASM International, Metal Park, Ohio, 1988) p. 679.
30. A. T. DIBENEDETTO and K. L. TRACHTE, *J. Appl. Polym. Sci.* **14** (1970) 2249.
31. K. FRIEDICH, L. A. CARLSSON, J. W. GILLESPIE, JR. and J. KARGER-KOCSIS, "Thermoplastic Composite Materials" (Elsevier Science Publisher, Amsterdam, 1991) p. 233.
32. D. R. MOORE, *Polym. Testing* **5** (1985) 255.

Received 27 February
and accepted 23 September 2003